Mercury anomaly, Deccan volcanism, and the end-Cretaceous mass extinction

Eric Font[1]*, Thierry Adatte[2], Alcides Nobrega Sial[3], Luiz Drude de Lacerda[4], Gerta Keller[5], and Jahnavi Punekar[5]

[1]IDL-FCUL (Instituto Dom Luís, Faculdade de Ciências da Universidade de Lisboa), Campo Grande, Edifício C1, Piso 1, 1749-016 Lisbon, Portugal

[2]ISTE (Institute of Earth Sciences), Geopolis, University of Lausanne, CH-1015 Lausanne, Switzerland

[3]NEG-LABISE (Nucleus of Geochemical Studies Stable Isotope Laboratory), Department of Geology, Federal University of Pernambuco, P.O. Box 7852, Recife, PE 50740-530, Brazil

[4]LABOMAR, Institute of Marine Sciences, Federal University of Ceará, Fortaleza, 60165-081, Brazil

[5]Department of Geosciences, Guyot Hall, Princeton University, Princeton, New Jersey 08544, USA

ABSTRACT

The contribution of the Deccan Traps (west-central India) volcanism in the Cretaceous-Paleogene (KPg) crisis is still a matter of debate. Recent U-Pb dating of zircons interbedded within the Deccan lava flows indicate that the main eruptive phase (>1.1 × 10^6 km^3 of basalts) initiated ~250 k.y. before and ended ~500 k.y. after the KPg boundary. However, the global geochemical effects of Deccan volcanism in the marine sedimentary record are still poorly resolved. Here we investigate the mercury (Hg) content of the Bidart (France) section, where an interval of low magnetic susceptibility (MS) located just below the KPg boundary was hypothesized to result from paleoenvironmental perturbations linked to the paroxysmal Deccan phase 2. Results show Hg concentrations >2 orders of magnitude higher from ~80 cm below to ~50 cm above the KPg boundary (maximum 46.6 ppb) and coincident with the low MS interval. Increase in Hg contents shows no correlation with clay or total organic carbon contents, suggesting that the Hg anomalies resulted from higher input of atmospheric Hg species into the marine realm, rather than organic matter scavenging and/or increased runoff. The Hg anomalies correlate with high shell fragmentation and dissolution effects in planktic foraminifera, suggesting correlative changes in marine biodiversity. This discovery represents an unprecedented piece of evidence of the nature and importance of the Deccan-related environmental changes at the onset of the KPg mass extinction.

INTRODUCTION

Large igneous province (LIP) volcanism is a possible cause in four of the five major mass extinctions in Earth history. However, this link remains controversial because for most LIPs there is no direct evidence of the mass extinction within the volcanic sequences. The Cretaceous-Paleogene (KPg) boundary is the most famous example where there is a direct correlation between the KPg mass extinction and both a meteorite impact and massive Deccan Traps (west-central India) volcanism within a very short geological time interval (Chenet et al., 2007; Renne et al., 2015; Schoene et al., 2015). The mass extinction in planktic foraminifera was documented between Deccan lava flows in the Krishna-Godavari Basin >1000 km from the Deccan Traps; these lava flows correspond to magnetochron C29r (Keller et al., 2011). On a global basis, quantification of the paleoclimatic and paleoenvironmental effects of volcanism and their impacts on and contributions to the KPg mass extinction remain a challenge. One potential method to investigate these global effects is to identify key exceptional sedimentary sequences that span the KPg mass extinction interval. With such sections changes in key proxy

elements such as mercury (Hg), which have been identified as possible markers for LIPs (e.g., Grasby et al., 2015), can be assessed and discussed in the context of both the meteorite impact and volcanism.

Here we investigate the Hg composition of the Bidart (France) section (Fig. 1), considered one of the most complete KPg sections worldwide (Bonté et al., 1984; Font et al., 2014; Galbrun and Gardin, 2004), and where an interval of low magnetic susceptibility (MS) resulting from partial dissolution of detrital magnetite and disappearance of biogenic magnetite (magnetofossil) was hypothesized to be driven by paleoenvironmental perturbations induced by Deccan volcanism (Abrajevitch et al., 2015; Font et al., 2014). This peculiar interval of low MS, also observed in Gubbio (Italy) (Ellwood et al.,
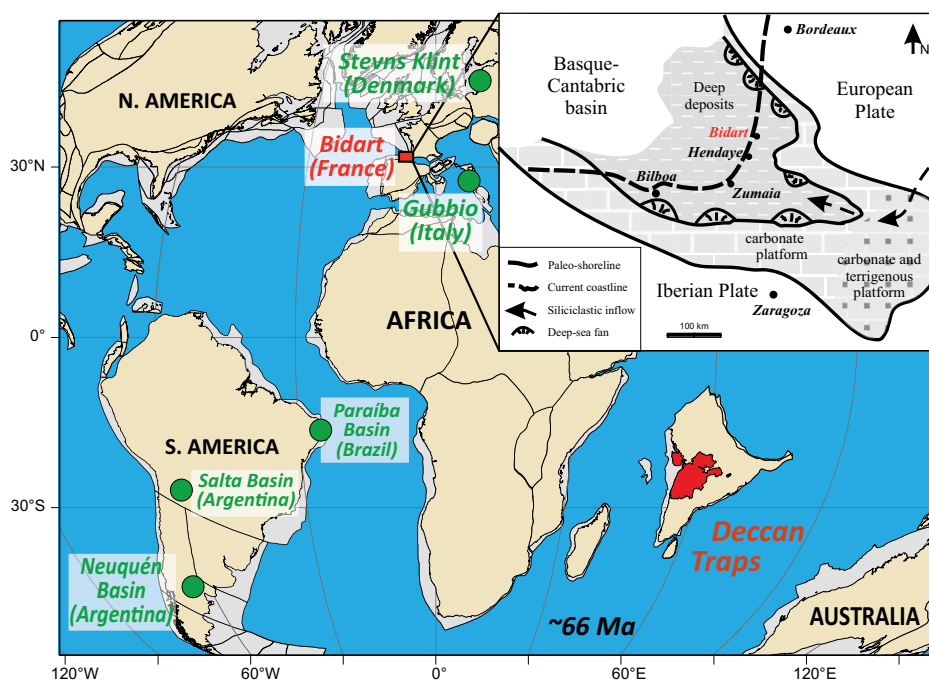
Figure 1. Paleogeographic map at the Cretaceous-Paleogene (KPg) transition (ca. 66 Ma) showing the locations of the studied area and the Deccan Traps (Trond Torsvik, 2015, personal commun.). Gray shelf areas correspond to present-day submerged extended crust. Locations of KPg sections where Hg anomalies have been documented are shown in green (see references in the text). The inset shows the paleogeographic map of the Basque-Cantabric Basin and the location of the Bidart section.

*E-mail: font_eric@hotmail.com

2003), is in the uppermost part of biozone CF1 just below the KPg boundary (Font et al., 2014) and is correlative with the onset of the most intense Deccan eruptions of phase 2 (Schoene et al., 2015) (Fig. 2). On a global basis, this interval also correlates with a negative excursion in osmium isotopes observed in multiple sections worldwide and attributed to weathering of Deccan lava flows (Robinson et al., 2009).

Mercury emissions are of global interest due to extreme toxicity, relatively long residence time, and long-range atmospheric transport ability (Percival et al., 2015, and references therein). The major reservoir on Earth is the global ocean, with Hg input from volcanic emissions and natural and anthropogenic coal combustion. Meteorites may have significant Hg contents (mostly as HgS after thermal release at ~340 °C), but quantification remains problematic due to uncertainties in analytical methods (Lauretta et al., 2001). Most volcanic Hg is emitted as gaseous elemental mercury (Hg^0), albeit as constrained by passive degassing (eruptions are less well constrained), that has residence times in the atmosphere of 0.5–2 yr, providing Hg^0 the ability to be transported globally away from its initial source (Bagnato et al., 2011; Pyle and Mather, 2003; Witt et al., 2008). Hg^0 is further removed from the atmosphere through oxidation by radicals (halogens, ozone) to form reactive Hg^{2+}, which is soluble in water and prone to deposition by rainfall.

Mechanisms responsible for subsequent Hg sequestration in sediments are rather complex, but generally rely on the formation of organic Hg-rich complexes. Covariation between Hg contents and organic matter in modern and ancient sediments suggests that Hg deposition rates are controlled by variations in biologic productivity and organic matter burial (e.g., Grasby et al., 2013; Outridge et al., 2007; Sanei et al., 2012). Alternatively, Hg can be adsorbed onto clays (Krupp, 1988). Covariation between Hg and Al_2O_3 observed in some sections across the KPg also suggests that Hg was probably adsorbed onto continental clays with subsequent transport and deposition into the ocean realm (Sial et al., 2013).

Maximum Hg deposition rates in recorded history, following the Indonesian Tambora (A.D. 1815) and Krakatau (A.D. 1883) eruptions and preserved in the glacial ice core of Upper Fremont Glacier (Wyoming, USA), reached 15×10^3 and 25×10^3 ppb, respectively, equivalent to 18× background deposition rates (Schuster et al., 2002). Major Hg fluctuations (maximum 116 ppb) linked to Siberian Traps volcanism have been observed across the Permian–Triassic biotic crises (Grasby et al., 2013; Sanei et al., 2012). Grasby et al. (2015) estimated that the Siberian Traps may have released up to 9.98 Gg yr^{-1} Hg (for a sporadic eruption rate over 40 k.y.), equivalent to 400% above modern natural emissions. Hg-rich levels

also feature in the records of the latest Pliensbachian–Toarcian oceanic anoxic event and have been linked to the Karoo-Ferrar LIP (primarily South Africa and Antarctica), although considerable variability between sections is observed on a global basis (Percival et al., 2015). Anomalous Hg concentrations have also been reported from end-Cretaceous–Paleogene sediments in Brazil, Argentina, Denmark, and Italy, and attributed to the Deccan Traps (Sial et al., 2013, 2014; Silva et al., 2013). However, Hg anomalies show strong variability among sections and lack of normalization against total organic carbon (TOC); this limits their correlation on a global scale. Therefore, Hg concentrations analyzed here are normalized to TOC and phyllosilicate content to determine whether the observed increase reflects increased organic matter sequestration and/or runoff processes or increased Hg deposition from atmospheric Deccan volcanic emissions.

MATERIALS AND METHODS

The Bidart section crops out in the Erretegia beach (43.46ºN, 1.58ºW, at sea level), in the Basque-Cantabric Basin (southwest France), and consists of hemipelagic to pelagic sediments deposited in a deep basin. The Maastrichtian section (latest Cretaceous) is dominated by marls and calcareous marls, whereas Danian (earliest Paleogene) sediments are composed of pink and white biogenic limestone beds.
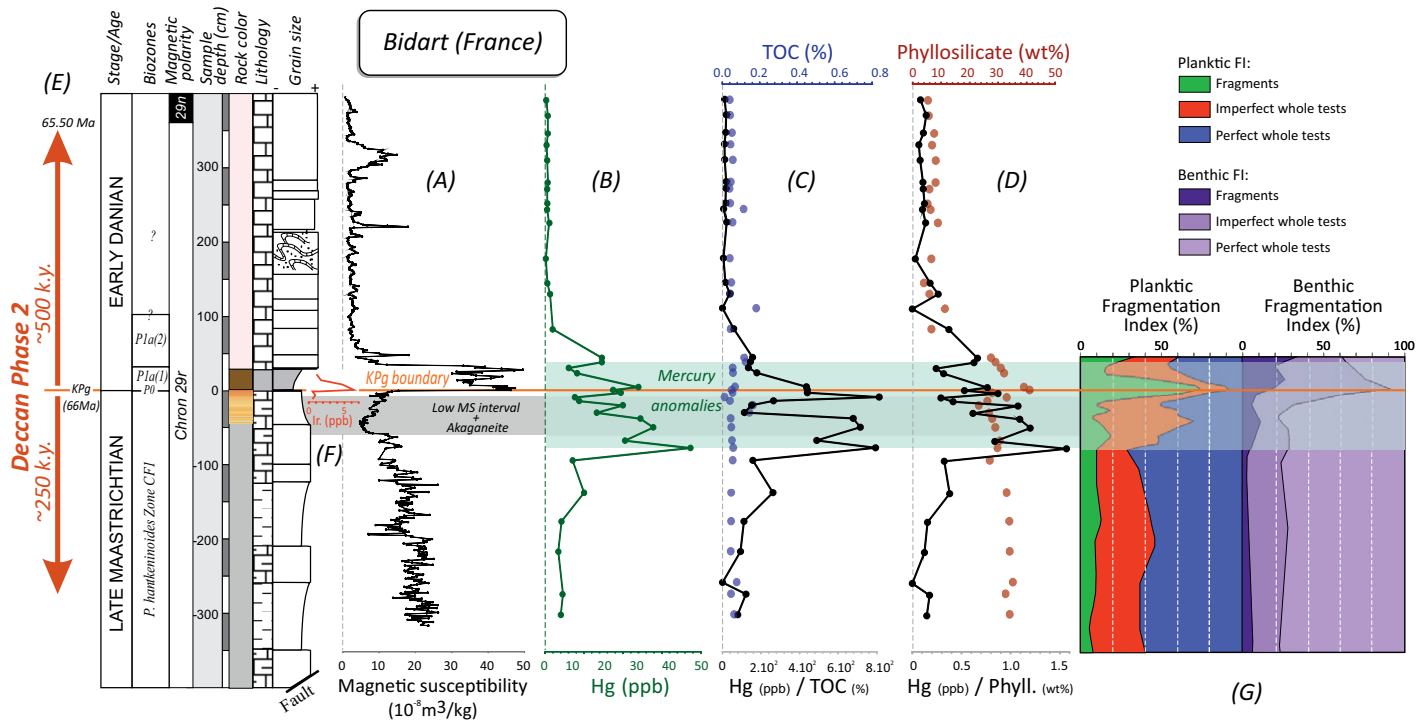
Figure 2. A: Magnetic susceptibility (MS) of the Cretaceous-Paleogene (KPg) transition at Bidart (Font et al., 2011). B: Hg concentration. C: Total organic carbon (TOC) and Hg/TOC ratio. D: Phyllosilicate contents and Hg/phyllosilicate (Phyll.) ratio. E: Ages of Deccan phase 2 (Schoene et al., 2015). *P.—Plummerita*. F: The iridium (Ir) anomaly (Bonté et al., 1984). G: Planktic and benthic fragmentation indexes (FI; Punekar et al., 2015).

Hg analyses were conducted in the same samples previously analyzed in Font et al. (2011). Hg content was determined at the University of Lausanne (Switzerland) using the Zeeman R-915F (Lumex, St. Petersburg, Russia), a high-frequency atomic absorption spectrometer specifically designed for Hg determination with a detection limit of 0.3–3 ppb (described in Percival et al., 2015). Measurements are based on the direct thermal evaporation of Hg from solid samples and do not require chemical pretreatment of samples, thus avoiding potential contamination during sample preparation. Analyses were conducted on two aliquots. The accuracy was confirmed by the analysis of certified reference materials (Chinese alluvium GSD-11 [Zintwana et al., 2012]; Hg content of 72.0 ppb). Excellent correspondence to the certified values was obtained with a correlation coefficient of 0.99 and a standard residual deviation of 0.44.

Total organic carbon analyses were carried out with a Rockeval 6 and quantified by flame ionization and infrared detection (±0.14% error). Mineralogical analyses were carried out with a Thermo Scientific ARL X'TRA diffractometer (±10% error). TOC and mineralogical analyses were performed at the University of Lausanne, Switzerland.

RESULTS AND DISCUSSION

Our results at Bidart show Hg concentrations two orders of magnitude higher in the stratigraphic interval beginning 20 cm below the onset of the low MS interval and 80 cm below the KPg boundary (Fig. 2; data are available in Table DR1 and Fig. DR1 in the GSA Data Repository[1]). The onset of Hg concentrations is abrupt (46.6 ppb), then gradually decreases to background values (<0.1 ppb) in the early Danian zone P1a(2) ~50 cm above the KPg boundary (Fig. 2).

At Bidart, latest Maastrichtian and early Danian sediments show low TOC contents (<0.16%; see Table DR1), although subtle increases are noted just below the KPg boundary and at 100 cm above (Fig. 2). After normalizing Hg concentrations by TOC values, there is no significant correlation in the Maastrichtian samples and at the KPg boundary, suggesting that Hg peaks are not linked to organic matter scavenging.

Clay minerals are the alternative host for scavenging Hg in marine sediments via adsorption and subsequent deposition on the ocean seafloor. At Bidart, clay mineral concentrations are quantified based on phyllosilicate contents, which average 30% of the bulk mineralogy during the latest Maastrichtian (zone CF1), increase to 41% at the KPg boundary, and decrease grad-

ually to <10% in the earliest Danian (Fig. 2; see Table DR1). Correlation between phyllosilicate content and Hg concentrations is poor, indicating that Hg fluctuations are not controlled primarily by clay content, even if some Hg is probably adsorbed onto clay. The strong noncorrelative trends of Hg, TOC, and phyllosilicate through time suggest that the Hg anomalies are not linked to increased organic matter burial and/or runoff. Such negative or noncorrelative trends between Hg and TOC have also been observed at the Permian-Triassic boundary and linked to Siberian Traps activity (Grasby et al., 2013; Sanei et al., 2012).

The Hg anomalies are found within sedimentary layers overlapping the ~50-cm-thick low MS interval and spanning the KPg boundary (Fig. 2). Whether the Chicxulub (Yucatan, Mexico) impact contributed to the Hg anomalies observed here and worldwide is still an open question, but the absence of impact markers and iridium anomalies in the interval of interest at Bidart (Bonté et al., 1984), just below and above the KPg boundary, argues for a major contribution from the Deccan Traps (Fig. 2). The low MS interval has been identified in two distal marine realms, at Bidart (Atlantic) and Gubbio (Tethys), suggesting a widespread signature (Font et al., 2011), although this still has to be confirmed by at other localities. This signal resulted from partial dissolution of detrital magnetite and total absence of biogenic magnetite, features consistent with changes in redox conditions, including ocean acidification and acid rains (Abrajevitch et al., 2015; Font et al., 2014). The presence of akaganeite (β-FeOOH-Cl) in the low MS of both sections, hypothesized to be of a volcanic origin, is further evidence of these peculiar paleoenvironmental conditions (Font et al., 2014).

On a global basis, the Hg anomaly documented here is correlative with similar anomalies reported worldwide (Sial et al., 2013), albeit with considerable variability among sections in term of Hg concentrations and stratigraphic position (Fig. 1). However, low sample resolution at these KPg intervals made any correlation with the low MS interval of Bidart uncertain. In summary, the close association of high Hg contents, iron oxide dissolution, and presence of akaganeite at Bidart strongly argue for widespread paleoenvironmental and paleoclimate perturbation induced by Deccan phase 2 volcanism across the KPg boundary.

Deccan magmas are estimated to release as much as 6 ± 1.7 Mt of SO_2 km^{-3} (Self et al., 2014). Assuming a volume of 1.1×10^6 km^3 of basalt erupted within the 750 k.y. of magnetochron C29r that encompass Deccan phase 2 (Schoene et al., 2015), the total SO_2 release would approximate 4.73–8.47×10^6 Mt, which corresponds to a total Hg input of 99.3–177.8 Mt (considering the Hg/SO_2 ratio of $0.21 \times 10^{-}$

[4]; Nriagu, 1989). For comparison, estimates of Hg released by the Chicxulub impact do not exceed 0.4 ± 0.2 Mt (Sial et al., 2013). These huge amounts of volcanic Hg emitted into the atmosphere readily explain the Hg anomalies recorded here and in other KPg sections. Although the role of Hg in the KPg mass extinction is still unknown, it may have poisoned both marine and continental waters. Clues to possible Hg effects are observed at Bidart, where Hg-enhanced intervals correlate with high planktic foraminiferal dissolution evident in shell fragmentation (10%–20%) and imperfect tests with holes (50%–70%) (Punekar et al., 2016; Fig. 2). In contrast, benthic assemblages show significantly lower test fragmentation (<10%) and imperfect tests (20%–30%). On a global basis, high-stress conditions in zones CF1 and CF2 below the KPg are correlative with Deccan volcanism phase 2 and have been documented in planktic foraminifera by including species dwarfing, diversity decrease, and dominance of disaster opportunist species (Keller et al., 2016).

Another stress marker possibly associated with Hg is biogenic magnetite produced by magnetotactic bacteria, which are controlled by the position of the anoxic-oxic boundary interface in the water or sediment columns (Moskowitz et al., 2008). These bacteria are particularly sensitive to changes in redox conditions, as reflected by their absence in the low MS intervals of the Bidart and Gubbio sections (Abrajevitch et al., 2015). However, they are present at the KPg boundary in both sections, suggesting that the Chicxulub impact had no environmental effects on their life and preservation. Therefore, these biodiversity proxies, together with the newly found Hg anomalies, provide new and promising clues to unravel the contribution of Deccan phase 2 volcanism in the end-Cretaceous mass extinction.

CONCLUSIONS

We report anomalous concentrations of Hg in the KPg section at Bidart within stratigraphic layers correlative with the major Deccan eruption episode, phase 2. The absence of correlation between Hg anomalies and organic matter and/or clay content (phyllosilicate) indicates a volcanic origin, probably via deposition of atmospheric Hg species into the oceanic realm, rather than via scavenging organic matter and/or increase in runoff processes. The Hg-enhanced level spans from 80 cm below the KPg to 50 cm above into the early Danian and encompasses an ~50-cm-thick interval of low MS below the KPg boundary. The Hg anomalies and low MS interval correlate with a high fragmentation index in planktic foraminifera, suggesting that the associated paleoenvironmental and paleoclimate perturbations had significant effects on biodiversity in marine calcifers. Thus, our study supports the use of Hg as a valuable volcanic

LIP indicator and highlights its importance in the Deccan-related environmental changes at the onset of the KPg mass extinction.

REFERENCES CITED
Abrajevitch, A., Font, E., Florindo, F., and Roberts, A.P., 2015, Asteroid impact vs. Deccan eruptions: The origin of low magnetic susceptibility beds below the Cretaceous-Paleogene boundary revisited: Earth and Planetary Science Letters, v. 430, p. 209–223, doi:10.1016/j.epsl.2015 .08.022.

Bagnato, E., Aiuppa, A., Parello, F., Allard, P., Shinohara, H., Liuzzo, M., and Giudice, G., 2011, New clues on the contribution of Earth's volcanism to the global mercury cycle: Bulletin of Volcanology, v. 73, p. 497–510, doi:10.1007 /s00445-010-0419-y.

Bonté, P., Delacotte, O., Renard, M., Laj, C., Boclet, D., Jehanno, C., and Rocchia, R., 1984, An iridium rich layer at the Cretaceous-Tertiary boundary in the Bidart section (southern France): Geophysical Research Letters, v. 11, p. 473–476, doi:10.1029/GL011i005p00473.

Chenet, A.L., Quidelleur, X., Fluteau, F., Courtillot, V., and Bajpai, S., 2007, ^{40}K-^{40}Ar dating of the main Deccan large igneous province: Further evidence of KTB age and short duration: Earth and Planetary Science Letters, v. 263, p. 1–15, doi:10.1016/j.epsl.2007.07.011.

Ellwood, B.B., MacDonald, W.D., Wheeler, C., and Benoist, S.L., 2003, The K/T boundary in Oman: Identified using magnetic susceptibility field measurements with geochemical confirmation: Earth and Planetary Science Letters, v. 206, p. 529–540, doi:10.1016/S0012-821X (02)01124-X.

Font, E., Nedelec, A., Ellwood, B.B., Mirao, J., and Silva, P.F., 2011, A new sedimentary benchmark for the Deccan Traps volcanism?: Geophysical Research Letters, v. 38, L24309, doi:10.1029 /2011GL049824.

Font, E., Fabre, S., Nedelec, A., Adatte, T., Keller, G., Veiga-Pires, C., Ponte, J., Mirão, J., Khozyem, H., and Spangenberg, J., 2014, Atmospheric halogen and acid rains during the main phase of Deccan eruptions: Magnetic and mineral evidence, in Keller, G., and Kerr, A.C., eds., Volcanism, impacts, and mass extinctions: Causes and effects: Geological Society of America Special Paper 505, p. 353–368, doi:10.1130/2014.2505(18).

Galbrun, B., and Gardin, S., 2004, New chronostratigraphy of the Cretaceous-Paleogene boundary interval at Bidart (France): Earth and Planetary Science Letters, v. 224, p. 19–32, doi:10.1016/j .epsl.2004.04.043.

Grasby, S.E., Sanei, H., Beauchamp, B., and Chen, Z.H., 2013, Mercury deposition through the Permo-Triassic biotic crisis: Chemical Geology, v. 351, p. 209–216, doi:10.1016/j.chemgeo .2013.05.022.

Grasby, S.E., Beauchamp, B., Bond, D.P.G., Wignall, P., and Sanei, H., 2015, Mercury anomalies associated with three extinction events (Capitanian crisis, latest Permian extinction and the Smithian/Spathian extinction) in NW Pangea: Geological Magazine, 13 p., doi:10.1017/S0016756815000436.

Keller, G., Bhowmick, P.K., Upadhyay, H., Dave, A., Reddy, A.N., Jaiprakash, B.C., and Adatte, T., 2011, Deccan volcanism linked to the Cretaceous-Tertiary mass extinction: New evidence from ONGC wells in the Krishna-Godavari Basin: Geological Society of India Journal, v. 78, p. 399–428, doi:10.1007/s12594-011-0107-3.

Keller, G., Punekar, J., and Mateo, P., 2016, Upheavals during the late Maastrichtian: Volcanism, climate and faunal events preceding the end-Cretaceous mass extinction: Palaeogeography, Palaeoclimatology, Palaeoecology, v. 441, p. 137–151, doi:10.1016/j.palaeo.2015.06.034.

Krupp, R., 1988, Physicochemical aspects of mercury metallogenesis: Chemical Geology, v. 69, p. 345–356, doi:10.1016/0009-2541(88)90045-9.

Lauretta, D.S., Klaue, B., Blum, J.D., and Buseck, P.R., 2001, Mercury abundances and isotopic compositions in the Murchison (CM) and Allende (CV) carbonaceous chondrites: Geochimica et Cosmochimica Acta, v. 65, p. 2807–2818, doi:10.1016/S0016-7037(01)00630-5.

Moskowitz, B.M., Bazylinski, D.A., Egli, R., Frankel, R.B., and Edwards, K.J., 2008, Magnetic properties of marine magnetotactic bacteria in a seasonally stratified coastal pond (Salt Pond, MA, USA): Geophysical Journal International, v. 174, p. 75–92, doi:10.1111/j.1365-246X .2008.03789.x.

Nriagu, J.O., 1989, A global assessment of natural sources of atmospheric trace metals: Nature, v. 338, p. 47–49, doi:10.1038/338047a0.

Outridge, P.M., Sanei, H., Stern, G.A., Hamilton, P.B., and Goodarzi, F., 2007, Evidence for control of mercury accumulation rates in Canadian High Arctic lake sediments by variations of aquatic primary productivity: Environmental Science & Technology, v. 41, p. 5259–5265, doi:10.1021 /es070408x.

Percival, L.M.E., Witt, M.L.I., Mather, T.A., Hermoso, M., Jenkyns, H.C., Hesselbo, S.P., Al-Suwaidi, A.H., Storm, M.S., Xu, W., and Ruhl, M., 2015, Globally enhanced mercury deposition during the end-Pliensbachian extinction and Toarcian OAE: A link to the Karoo–Ferrar large igneous province: Earth and Planetary Science Letters, v. 428, p. 267–280, doi:10.1016/j.epsl .2015.06.064.

Punekar, J., Keller, G., Khozyem, H., Adatte, T., Font, E., and Spangenberg, J., 2015, A multiproxy approach to decode the end-Cretaceous mass extinction: Paleogeography, Paleoclimatology, Paleoecology, v. 441, p. 116–136, doi: 10.1016/j.palaeo.2015.08.025.

Pyle, D.M., and Mather, T.A., 2003, The importance of volcanic emissions for the global atmospheric mercury cycle: Atmospheric Environment, v. 37, p. 5115–5124, doi:10.1016/j.atmosenv .2003.07.011.

Renne, P., Sprain, C.J., Richards, M.A., Self, S., Vanderkluysen, L., and Pande, K., 2015, State shift in Deccan volcanism at the Cretaceous-Paleogene boundary, possibly induced by impact: Science, v. 350, p. 76–78, doi:10.1126/science.aac7549.

Robinson, N., Ravizza, G., Coccioni, R., Peucker-Ehrenbrink, B., and Norris, R., 2009, A high-resolution marine $^{187}Os/^{188}Os$ record for the late Maastrichtian: Distinguishing the chemical fingerprints of Deccan volcanism and the KP impact event: Earth and Planetary Science Letters, v. 281, p. 159–168, doi:10.1016/j.epsl.2009.02.019.

Sanei, H., Grasby, S.E., and Beauchamp, B., 2012, Latest Permian mercury anomalies: Geology, v. 40, p. 63–66, doi:10.1130/G32596.1.

Schoene, B., Samperton, K.M., Eddy, M.P., Keller, G., Adatte, T., Bowring, S.A., Khadri, S.F.R., and Gertsch, B., 2015, U-Pb geochronology of the Deccan Traps and relation to the end-Cretaceous mass extinction: Science, v. 347, p. 182–184, doi:10.1126/science.aaa0118.

Schuster, P.F., Krabbenhoft, D.P., Naftz, D.L., Cecil, L.D., Olson, M.L., Dewild, J.F., Susong, D.D., Green, J.R., and Abbott, M.L., 2002, Atmospheric mercury deposition during the last 270 years: A glacial ice core record of natural and anthropogenic sources: Environmental Science & Technology, v. 36, p. 2303–2310, doi:10.1021 /es0157503.

Self, S., Schmidt, A., and Mather, T.A., 2014, Emplacement characteristics, time scales, and volcanic gas release rates of continental flood basalt eruptions on Earth, in Keller, G., and Kerr, A.C., eds., Volcanism, impacts, and mass extinctions: Causes and effects: Geological Society of America Special Paper 505, p. 319–337, doi:10.1130 /2014.2505(16).

Sial, A.N., Lacerda, L.D., Ferreira, V.P., Frei, R., Marquillas, R.A., Barbosa, J.A., Gaucher, C., Windmoller, C.C., and Pereira, N.S., 2013, Mercury as a proxy for volcanic activity during extreme environmental turnover: The Cretaceous-Paleogene transition: Palaeogeography, Palaeoclimatology, Palaeoecology, v. 387, p. 153–164, doi:10.1016/j.palaeo.2013.07.019.

Sial, A.N., et al., 2014, High-resolution Hg chemostratigraphy: A contribution to the distinction of chemical fingerprints of the Deccan volcanism and Cretaceous-Paleogene Boundary impact event: Palaeogeography, Palaeoclimatology, Palaeoecology, v. 414, p. 98–115, doi:10.1016/j .palaeo.2014.08.013.

Silva, M.V.N., Sial, N.A., Barbosa, J.A., Ferreira, V.P., Neumann, V.H., and de Lacerca, L.D., 2013, Carbon isotopes, rare-earth elements and mercury geochemistry across the K-T transition of the Paraíba Basin, northeastern Brazil: Geological Society of London Special Publication 382, p. 85–104, doi:10.1144/SP382.2.

Witt, M.L.I., Mather, T.A., Pyle, D.M., Aiuppa, A., Bagnato, E., and Tsanev, V.I., 2008, Mercury and halogen emissions from Masaya and Telica volcanoes, Nicaragua: Journal of Geophysical Research, v. 113, B06203, doi:10.1029/2007JB005401.

Zintwana, M.P., Cawthorn, R.G., Ashwal, L.D., Roelofse, F., and Cronwright, H., 2012, Mercury in the Bushveld Complex, South Africa, and the Skaergaard Intrusion, Greenland: Chemical Geology, v. 320, p. 147–155, doi:10.1016/j .chemgeo.2012.06.001.